Local and global approaches to treat the torsional barriers of 4-methylacetophenone using microwave spectroscopy

Sven Herbers, Sean M Fritz, Piyush Mishra, Ha Vinh Lam Nguyen, Timothy S Zwier

The Journal of Chemical Physics

Local and global approaches to treat the torsional barriers of 4-methylacetophenone using microwave spectroscopy

Cite as: J. Chem. Phys. **152**, 074301 (2020); https://doi.org/10.1063/1.5142401
Submitted: 12 December 2019 . Accepted: 27 January 2020 . Published Online: 18 February 2020

Sven Herbers, Sean M. Fritz, Piyush Mishra, Ha Vinh Lam Nguyen, and Timothy S. Zwier

The Journal of Chemical Physics ARTICLE scitation.org/journal/jcp

Local and global approaches to treat the torsional barriers of 4-methylacetophenone using microwave spectroscopy

Cite as: J. Chem. Phys. 152, 074301 (2020); doi: 10.1063/1.5142401
Submitted: 12 December 2019 • Accepted: 27 January 2020 •
Published Online: 18 February 2020

Sven Herbers,[1] Sean M. Fritz,[1] Piyush Mishra,[1] Ha Vinh Lam Nguyen,[2,a)] and Timothy S. Zwier[1,a),b)]

AFFILIATIONS

[1] Department of Chemistry, Purdue University, 560 Oval Drive, West Lafayette, Indiana 47907, USA
[2] Laboratoire Interuniversitaire des Systèmes Atmosphériques (LISA), CNRS UMR 7583, Université Paris-Est Créteil, Université de Paris, Institute Pierre Simon Laplace, 61 avenue du Général de Gaulle, Créteil, France

[a)] **Authors to whom correspondence should be addressed:** lam.nguyen@lisa.u-pec.fr and zwier@purdue.edu
[b)] **Current address:** Combustion Research Facility, Sandia National Laboratories, Livermore, CA 94551-0969, USA.

ABSTRACT

The Fourier transform microwave spectrum of 4-methylacetophenone recorded from 8 GHz to 18 GHz under jet-cooled conditions has revealed large tunneling splittings arising from a low barrier to internal rotation of the ring methyl group and small splittings from a high torsional barrier of the acetyl methyl group. The large splittings are especially challenging to model, while the small splittings are difficult to analyze due to the resolution limit of 120 kHz. The combination of two methyl groups undergoing internal rotations caused each rotational transition to split into five torsional species, which were resolved and fitted using a modified version of the *XIAM* code and the newly developed *ntop* code to a root-mean-square deviation close to measurement accuracy, providing an estimate of the V_3 potential barriers of about 22 cm^{-1} and 584–588 cm^{-1} for the ring and the acetyl methyl groups, respectively. The assignment was aided by separately fitting the five torsional species using odd-power order operators. Only one conformer in which all heavy atoms are located on a symmetry plane could be identified in the spectrum, in agreement with results from conformation analysis using quantum chemical calculations.

I. INTRODUCTION

The potentials of methyl internal rotation in toluene derivatives provide fascinating insights into the electronic structure effects of substitution. In this sense, the methyl rotor is an exquisite probe of its local electronic environment. It is known that the potential of methyl internal rotation in toluene (**1**) consists of a pure V_6 term due to the C_{3v} symmetry of the methyl group and the C_{2v} symmetry of the phenyl ring (for molecule numbering, see Fig. 1).[1] The shape and height of this potential vary strongly if further substituents are added on the ring, which often breaks the C_{2v} symmetry of the phenyl ring so that a V_3 term occurs. Figure 1 summarizes the experimental methyl rotor barriers in a series of substituted toluenes that illustrate this point. A systematic microwave study on three isomers of methylanisole has shown that the V_3 potential is largest when the methoxy substituent is located next to the methyl group of toluene (444 cm^{-1})[2] but decreases drastically when it is in the *meta*[3] and *para*-position[4] (**8**) of the ring with respective values of 55.7693(90) cm^{-1} and 49.6370(1) cm^{-1}. In fluoro- and chlorotoluene, the same trend was observed, where the V_6 potential of toluene becomes an almost pure V_3 potential in *o*-fluoro and *o*-chlorotoluene with barrier heights of 227.28(2)[5] and 513.8(27) cm^{-1},[6] respectively, but stays a pure V_6 potential in *p*-fluoro (**2**)[7] and *p*-chlorotoluene (**3**)[8] with almost the same barrier height as that of toluene. Substitution at the *para*-position of toluene produces a low barrier to methyl torsion, which is confirmed by the study on *p*-toluic acid (**6**) with a V_3 term of 7.899(1) cm^{-1} and a V_6 leading term of −24.77(2) cm^{-1} in the potential.[9] The V_3/V_6 ratio as well as their signs are in agreement with results from theoretical calculations at the MP2/6-311++G(2d,p) level of theory; and fitting both V_3 and V_6 is required to obtain a reasonable fit.[9] In the investigation on *p*-tolualdehyde (**5**), Saal *et al.* reported a V_3 potential of

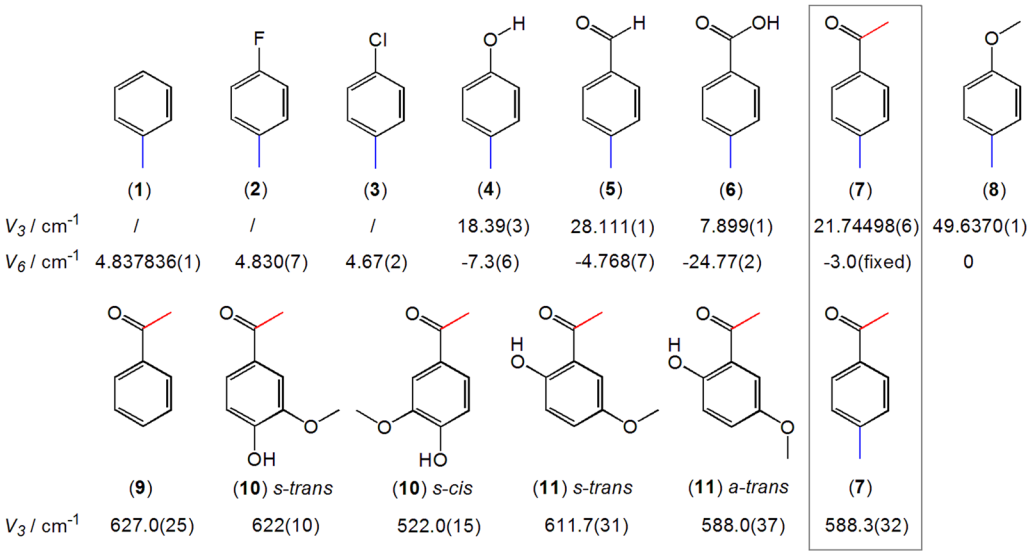

FIG. 1. A selection of molecules featuring methyl internal rotation(s) related to 4-methylacetophenone. Upper trace: potential barriers of the *p*-methyl group (blue) in substituted toluenes: (1) toluene,[1] (2) *p*-fluorotoluene,[7] (3) *p*-chlorotoluene,[8] (4) *p*-cresol,[11] (5) *p*-tolualdehyde,[10] (6) *p*-toluic acid,[9] (7) 4-methylacetophenone (this work), and (8) *p*-methylanisole.[4] Lower trace: V_3 potential of the acetyl methyl group (red) in substituted acetophenones: (9) acetophenone,[12] (10) acetovanillone,[13] and (11) 6-hydroxy-3-methoxyacetophenone.[13]

28.111(1) cm^{-1} with a V_6 contribution of −4.768(7) cm^{-1}.[10] Finally, in *p*-cresol (**4**), a barrier height of only 18.39(3) cm^{-1} has been observed.[11]

From the studies on *p*-tolualdehyde (**5**) and *p*-toluic acid (**6**), we see that the double bond of the carbonyl group contributes to π-conjugation throughout the phenyl ring and significantly affects methyl internal rotation.[9,10] This "long distance calling"[10] from the acid or the aldehyde group is felt by the methyl group at the other side of the phenyl ring. To learn more about this effect, it is interesting to study 4-methylacetophenone (**7**) (4MAP) where an acetyl group is attached at the *para*-position of toluene.

Another interesting aspect of 4MAP is that the methyl group in the acetyl moiety (hence forward called the acetyl methyl group) also undergoes internal rotation, but the torsional barrier is anticipated to be much higher than that of the ring methyl group. In acetophenone (**9**), the barrier height of the acetyl methyl torsion is 627.0(25) cm^{-1}.[12] In acetovanillone (**10**), Cocinero *et al.* reported a similar barrier of 622(10) cm^{-1} for the *s-trans* conformer and a lower barrier of 552.0(15) cm^{-1} for the *s-cis* conformer.[13] In the same work, the *s-trans*-conformer of 6-hydroxy-3-methoxyacetophenone (**11**) undergoes acetyl methyl internal rotation with a barrier height of 611.7(31) cm^{-1}, while the *a-trans* conformer has a slightly lower barrier of 588.0(37) cm^{-1}.[13] Obviously, the barrier to internal rotation of the acetyl methyl group changes with conformation and isomer but remains around 600 cm^{-1}. Recently, Andresen *et al.* proposed a rule to predict the torsional barrier of the acetyl methyl group in aliphatic ketones, where the barrier height could be linked to the structure at the other side of the carbonyl group.[14] The linear aliphatic ketones under study were classified into two categories, the "C_s class" where the barrier is always around 180 cm^{-1} and the "C_1 class" with a barrier of approximately 240 cm^{-1}. Information on the torsional barrier of the acetyl methyl group of 4MAP (**7**) will provide new data to expand this "two-class concept" proposed for aliphatic ketones to also include phenyl-containing ketones.

Since 4MAP combines two methyl internal rotors in one molecule, we can probe whether the two interact through π-conjugation in the ring. Several molecules with two methyl rotors have been studied in the past, with acetone[15] and methyl acetate[16] as two classic examples. Other two-rotor molecules involving an aromatic ring have also been reported, such as 2,5-dimethylthiophene,[17] 2,5-dimethylfuran,[18] 2-acetyl-5-methylfuran,[19] dimethylbenzaldehyde,[20] and a series of dimethylanisoles.[21–23]

In many such molecules, the spectra are hard to assign and to model because development of new theoretical tools involving effective Hamiltonians is often required to reproduce the experimental spectra. A popular and widely used program for simulating microwave spectra of molecules with multiple methyl rotors is *XIAM*, written by Hartwig,[24,25] which can treat the effects of internal rotation with up to three methyl tops. *XIAM* is user-friendly and fast but has a drawback in its treatment of low barrier rotors, where higher order perturbation effects often have to be considered. High order terms are included in two-top programs written by Groner,[26] Ohashi,[27] Kleiner,[28] and Ilyushin.[29] Recently, a new code called *ntop* was developed, which works in the principal axis system and can fit the torsion–rotation spectra of molecules with *n* non-equivalent or equivalent methyl rotors. The equilibrium symmetry is not limited to C_s or C_{2v} but can also be C_1, and the number of high order terms is much higher than that in *XIAM*. When *ntop* was applied to 2,4-dimethylanisole,[23] it reduced the standard deviation of 24.1 kHz obtained by *XIAM* to 4.2 kHz, which is the measurement accuracy, by adding seven more effective parameters in the fit.

Another aspect of *XIAM* in treating low barrier rotation is its two-step diagonalization procedure, only considering one *J*-block in the second diagonalization step. This clearly affects fits, especially if strong quadrupole coupling is present in the system, as in the case of *meta*-chlorotoluene,[30] since in *XIAM*, the matrix elements off-diagonal in *J* are set to zero. Furthermore, the interaction between different v_t states is also not explicitly taken into account and some matrix elements are neglected, which could decrease the accuracy of the fit. Therefore, it is also argued that even if there were more effective terms in *XIAM*, the standard deviation would still be worse than with other programs. Using an internal rotation program called *aixPAM*, where the number of internal tops is limited to one (n = 1), and applying it on the spectra of *m*-methylanisole containing two conformers, this argument has been tested and proven false, and the work suggests that additional effective parameters in *XIAM* would allow fits with standard deviations close to measurement accuracy.[3] To test this prediction, we modified the *XIAM* program by including some higher order parameters that are not available in the original version of *XIAM* (see the PROSPE[31] website http://info.ifpan.edu.pl/kisiel/prospe.htm for downloading the original version of *XIAM*) to fit the microwave spectrum of 4MAP and compare the results with those from the *ntop* fit. We will see below that both programs provide fits to the full manifold of torsion–rotation transitions that are within measurement accuracy. This leads to a quantitative determination of both barrier heights in 4MAP for comparison with other members of the series in Fig. 1.

II. THEORY

A. Quantum chemical calculations

The structure of 4MAP was predicted using a geometry optimization at the B3LYP[32–35]-D3BJ[36–39]/def2TZVP[40,41] level of theory using Grimme's dispersion correction with Becke–Johnson damping as implemented in the *Gaussian 09* program package.[42] This level was chosen because of its cost-efficiency and qualitatively useful predictions of the microwave spectrum.

The optimized geometry of 4MAP is shown in Fig. 2. The calculated rotational constants are A = 3644.5 MHz, B = 788.5 MHz, and C = 653.4 MHz; and the dipole moment components are μ_a = 2.66 D, μ_b = 2.34 D, and μ_c = 0.00 D. The Gaussian 09 output is available in the supplementary material. Harmonic frequency calculations were carried out to predict the centrifugal distortion constants. Relaxed one-dimensional potential energy scans were performed along the torsional angles to predict the V_3 and V_6 terms with least squares fits of a Fourier series,

$$V_{\alpha_1}/\mathrm{cm}^{-1} = \frac{18.07}{2}(1-\cos(3\alpha_1)) - \frac{3.03}{2}(1-\cos(6\alpha_1)) + 0.101$$

and

$$V_{\alpha_2}/\mathrm{cm}^{-1} = \frac{452.48}{2}(1-\cos(3\alpha_2))$$

for the ring methyl and the acetyl methyl group, respectively, where α_1 and α_2 are the torsional angles of the methyl groups. The resulting functions are plotted in Fig. 3.

B. Symmetry considerations

G_{18} is the appropriate molecular symmetry group for 4MAP, which features C_s point-group symmetry at equilibrium and two inequivalent methyl groups undergoing internal rotation.[43] Recently, a labeling scheme, for which the G_{18} group is written as the semi-direct product $(C_3^I \otimes C_3^I) \ltimes C_s$, has been introduced for 3,4-dimethylanisole[22] and then applied for 2,4-dimethylanisole.[23] Using this scheme, the torsional species can be labeled by the first part $(\sigma_1\sigma_2)$ of the full symmetry label given in Table I of Ref. 22. We will also use this abbreviated notation (00), (01), (10), (11), and (12) for 4MAP, where σ_1 and σ_2 represent the ring and acetyl methyl groups, respectively. The numbers σ = 0, 1, 2 represent the three symmetry species A, E_a, and E_b, respectively, of the group C_3.

The two sets of three protons belonging to the two methyl groups and four protons attached on the phenyl ring result in 1024 spin functions. The representation of the total nuclear spin function is $\Gamma_{ns} = 256(00)\cdot A' + 128(10)\cdot A + 128(01)\cdot A + 64(11)\cdot A + 64(12)\cdot A$. The selection rules for torsional components are $(00)\cdot A' \leftrightarrow (00)\cdot A''$, $(10)\cdot A \leftrightarrow (10)\cdot A$, $(01)\cdot A \leftrightarrow (01)\cdot A$ with a

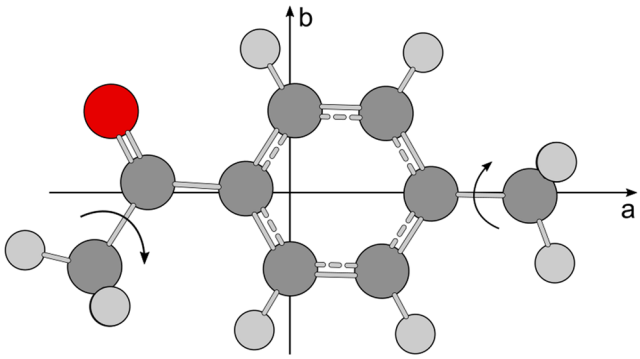

FIG. 2. Molecular structure of 4-methylacetophenone calculated at the B3LYP-D3BJ/def2TZVP level of theory, as viewed along the *c*-principal axis. This figure illustrates that (i) all heavy atoms are located on the *ab* plane and (ii) the ring methyl top is almost exactly parallel to the *a*-principal axis.

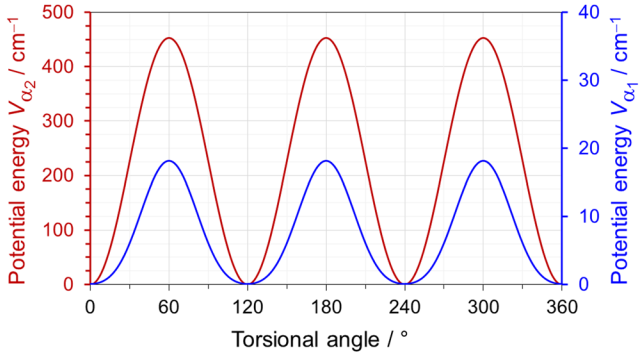

FIG. 3. Potential energy functions for the internal rotation of the ring methyl (blue) and the acetyl methyl group (red) of 4-methylacetophenone predicted at the B3LYP-D3BJ/def2TZVP level of theory. Energies relative to the lowest conformations with their absolute energies of E = −424.412 046 0 hartree are given.

TABLE I. Molecular parameters of 4-methylacetophenone as obtained with the program *XIAM* and *ntop*.

Parameters[a]	Unit	*XIAM*	*ntop*	$XIAM_{mod}$	Pred.[b]
A	MHz	3618.557 0(80)	3604.713 2(19)	3618.627 2(25)	3644.5
B	MHz	784.657 10(15)	784.646 59(30)	784.651 34(43)	788.5
C	MHz	650.444 0(11)	650.439 31(23)	650.441 96(30)	653.4
D_J	kHz	0.032 9(44)	0.014 00(93)	0.016 7(13)	0.0135
D_{JK}	kHz	0.004 312[c]	0.004 312[c]	0.004 312[c]	0.0043
D_K	kHz	−8.04(40)	0.37(11)	−0.86(17)	0.3347
d_1	kHz	−0.006 94(80)	0.003 39(16)	−0.003 66(24)	−0.0023
d_2	kHz	0.000 943[c]	0.000 943[c]	0.000 943[c]	0.0009
$V_{3,1}$	cm^{-1}	21.950 8 (55)	21.744 826(57)	21.947 9(13)	18.07
$V_{6,1}$	cm^{-1}	−3.027 9[c]	−3.027 9[c]	−3.027 9[c]	−3.03
$V_{3,2}$	cm^{-1}	594(24)	588.1(32)	583.6(66)	452.48
$D_{\pi 2J,1}$	MHz	0.001 43(34)	0.001 727(82)	0.001 563(98)	
$D_{\pi 2K,1}$	MHz	0.441 1(81)	0.940 628(69)	1.733(21)	
$D_{\pi 2-,1}$	MHz	0.000 18(21)	0.000 162(44)	0.000 179 (60)	
$V_{K,1}/-D_{c3K}$[d]	MHz		17.628 2(32)	11.943(19)	
$F_{0,1}$	GHz	161.29[c]	161.29[c]	161.29[c]	161.29
$F_{0,2}$	GHz	159.54[c]	159.54[c]	159.54[c]	159.54
δ_1	degree	0.771 7(61)	0.763 225(57)	0.765 5(18)	0.26
δ_2	degree	125.0(90)	123.0(32)	121.4(23)	122.98
N[e]		378	378	378	
rms[f]	kHz	99	26	29	

[a]Standard error in parentheses in the units of the last digits. Watson's S reduction and I^r representation were used.
[b]Values calculated at the B3LYP-D3BJ/def2TZVP level of theory.
[c]Fixed to the calculated value.
[d]$V_{K,1}$ in Fit *ntop* and D_{c3K} in Fit $XIAM_{mod}$.
[e]Number of assigned transitions in the fit.
[f]Root-mean-square deviation of the fit.

spin statistical weight of 256 and $(11)\cdot A \leftrightarrow (11)\cdot A$ and $(12)\cdot A \leftrightarrow (12)\cdot A$ with a spin weight of 128. If we only consider the spin statistical weight, the intensity of the (00), (10), and (01) species is twice of that of the (11) and (12) species.

C. The extended *XIAM* code

The *XIAM* code uses a combined axis method where the internal rotation Hamiltonian $H_{i,\mathrm{RAM}}$ is set up in the rho axis system and then rotated into the principal axis system using a rotation matrix,

$$\mathbf{D}(\beta,\gamma) = \begin{pmatrix} \cos\beta & 0 & -\sin\beta \\ 0 & 1 & 0 \\ \sin\beta & 0 & \cos\beta \end{pmatrix} \begin{pmatrix} \cos\gamma & \sin\gamma & 0 \\ -\sin\gamma & \cos\gamma & 0 \\ 0 & 0 & 1 \end{pmatrix}, \quad (1)$$

where β and γ are the Euler angles defined as $\cos(\beta) = \rho_z(\rho)^{-1}$ and $\cos(\gamma) = \rho_x((\rho_x)^2 + (\rho_y)^2)^{-0.5}$, where ρ is the coupling term and a vector parallel to the ρ-axis with its components ρ_x, ρ_y, and ρ_z in the principal axis system.[24,25]

XIAM can treat many top problems, but the basic Hamiltonian for a one-top problem can be written as

$$H = H_r + H_{cd} + D^{-1} H_{i,RAM} D, \quad (2)$$

where H_r is the rotational part of the Hamiltonian and H_{cd} is the centrifugal distortion term. Using this combined axis method, structural rotational constants are used in the fit, centrifugal distortion is treated in the principal axis system, and internal rotation parameters such as the angles δ between the internal rotor axes and the a-principal axis of inertia, the V_3 potentials, and F_0 (the rotational constants of the internal rotors) or ρ utilized in the fitting procedure are physically meaningful.

Currently, only a limited number of higher order parameters are available in *XIAM*. The three operators that are most efficient and frequently used are the internal rotation distortion terms $D_{\pi^2 J}$, $D_{\pi^2 K}$, and $D_{\pi^2 -}$, multiplying $2(p_\alpha - \vec{\rho}^{\dagger}\vec{P})^2 P^2$, $\{(p_\alpha - \vec{\rho}^{\dagger}\vec{P})^2, P_a^2\}$, and $\{(p_\alpha - \vec{\rho}^{\dagger}\vec{P})^2, (P_b^2 - P_c^2)\}$, respectively, where $\{A, B\} = AB + BA$ is the anti-commutator, p_α is the momentum operator of the internal rotation, and P is the angular momentum operator with its components P_a, P_b, and P_c.[44] They describe the dependence of the moment of inertia of the methyl rotor upon centrifugal distortion. The transformation of these operators into the equivalent operators in the principal axis system is complicated and is given in Table S1 of the supplementary material. Higher order terms describing the distortion of the potential surface along the torsional degree of freedom upon centrifugal distortion, connected to the potential term

$\cos(3\alpha)$, are limited to only one parameter, D_{c3J}, which multiplies the operator $\cos(3\alpha)P^2$.

In the study on 2,4-dimethylanisole, the program *ntop* reduced the standard deviation of 24.1 kHz obtained by *XIAM* to 4.2 kHz by adding seven effective parameters in the fit; among them, three higher order terms V_J, V_K, and V_- connected to the potential term $\cos(3\alpha)$ are decisive.[23] They multiply the operators $(1-\cos(3\alpha))P^2$, $\left(1-\cos(3\alpha)\right)P_a^2$, and $(1-\cos(3\alpha))(P_b^2-P_c^2)$, respectively. While the V_J operator of *ntop* is comparable to the D_{c3J} operator of *XIAM*, the V_K and V_- parameters are not available in *XIAM*. To make the performance of the two programs more comparable, we extended the *XIAM* code by modifying the source code to also include the D_{c3K} and D_{c3-} terms, which multiply $\cos(3\alpha)P_a^2$ and $\cos(3\alpha)(P_b^2-P_c^2)$. The results of a fit from this modified version of *XIAM* on 4MAP will be compared with those of *ntop* using the same set of transitions and comparable sets of parameters.

III. MICROWAVE SPECTROSCOPY

A. Experimental details

The microwave spectrum of 4MAP was recorded using a chirped-pulse Fourier transform microwave spectrometer at Purdue.[45] The sample (Alfa Aesar, 96%) was placed in a reservoir located just before a pulsed valve and heated up to 117 °C by a coiled resistive heater. Helium was used as carrier gas at an absolute backing pressure of 1.4 bars. Spectra were recorded in the range from 8 GHz to 18 GHz, acquiring 2 000 000 measurements of 16 μs that were averaged and then Fourier transformed. A Lorentz interpolation function was used to interpolate more precisely the center frequencies of the recorded transitions. In many rotational transitions, the torsional splittings between (00) and (01) as well as between (11)-(10)-(12) were below the resolution limit of 120 kHz of our instrument. In such cases, the frequencies were assigned only to (00) or (10), respectively. Two portions of the survey scan are illustrated in Fig. 4.

B. Spectral assignments

In an initial fit, only the (00) species was assigned to lines in the spectrum, yielding a fit with root-mean-square (rms) deviation of almost measurement accuracy using the program combination *SPFIT/SPCAT*.[46] The assignment was straightforward, and the (00) species lines followed the spectral patterns predicted using the rotational constants from the equilibrium geometry calculated at the B3LYP-D3BJ/def2TZVP level of theory.

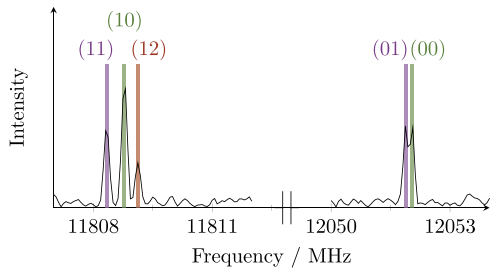

FIG. 4. Two typical spectra of the *b*-type Q-branches $J'_{K'_a,K'_c}-J''_{K''_a,K''_c}$ = 9_{28}–9_{19} transition of 4-methoxyacetophenone, which splits into five torsional components $(\sigma_1\sigma_2)$ = (00), (01), (10), (11), and (12).

To assign other torsional species, the calculated V_3 potentials (see Sec. II A) and angles δ between the internal rotor axes and the principal *a*-axis were used in a prediction with the program *XIAM*. For the value of δ, the internal rotation axis was identified to be parallel to a vector perpendicular to the plane of the three hydrogens in the optimized equilibrium structure. A fit with the initial assignment of the (10), (01), (11), and (12) species showed an rms deviation of several hundreds of kilohertz, assumed to be due to the misassignment of some torsional components.

The assignment of the individual torsional species was checked by a program written for *Separately Fitting of Large Amplitude Motion Species* (*SFLAMS*), similar to an approach used by Ohashi *et al.* to assign the microwave spectrum of *N*-methylacetamide.[27] These separate fits have established the assignments of rotational quantum numbers and of symmetry species, especially the (10), (11), and (12) components. For each fit, the Hamiltonian consists of

$$H = H_r + H_{cd} + H_{op}, \tag{3}$$

where

$$H_{op} = (q + q_J P^2 + q_K P_a^2)P_a + rP_b. \tag{4}$$

The odd power terms of the angular momentum components P_a and P_b change sign under the time-reversal operation. The Hamiltonian becomes effective and deviates from a normal Hamiltonian because the coefficients in H_{op} enclose numerical expectation values of an odd power of the torsional angular momentum operators of the methyl groups (p_α). However, if p_α were included explicitly in the torsion-rotational Hamiltonian, they would also change sign under time reversal, just as the odd power P_a, P_b, P_c operators. The sign changes cancel out, and the Hamiltonian H_{op} becomes invariant as it should be [see Eq. (4) of Ref. 27].

While H_{op} is not required to reproduce the (00) species of 4MAP, the q and r parameters (sometimes called D_a and D_b in the literature) are needed for the (01) species. For the (10), (11), and (12) species, the higher order terms q_J and q_K (or D_{aJ} and D_{aK}, respectively) are required in addition. In all separate fits, the deviations are about 25 kHz, indicating that this value is most probably the measurement accuracy.

C. Global fits

A total of 378 lines could be assigned with the aid of separate fits and were again included in the input of the program *XIAM*. With the correct assignment, the rms deviation of the *XIAM* fit decreases to 99 kHz by floating the rotational constants, three of five quartic centrifugal distortion constants, the V_3 potentials, the angles between the internal rotor axes and the *a*-principal axis, and three higher order parameters related to the low barrier top $D_{\pi^2 J}$, $D_{\pi^2 K}$, and D_{π^2-}. The parameters are collected in the column *XIAM* of Table I. The frequency list with all fitted transitions along with their residuals is available in Table S2 of the supplementary material. As can be seen in the frequency list, there are some *c*-type perturbation allowed transitions that occur because the quantum numbers K_a and K_c have no meaning for the symmetry of the rotational transitions apart from the (00) species. In the (01), (10), (11), and (12) species, the K_a and K_c quantum numbers only indicate the order of energy in analogy to the asymmetric top energy level.

The *ntop* code was applied using the same data set, where adding only one high order parameter of the low barrier ring methyl rotor, $V_{K,1}$, decreased the rms deviation to 26 kHz. The fit is shown in the column *ntop* of Table I. The residuals of all fitted transitions are also given in Table S2 of the supplementary material.

We then added the *XIAM*'s version of $-V_K$, called D_{c3K}, using the modified *XIAM* code, and the rms deviation was reduced to 29 kHz, which is close to the measurement accuracy and only 3 kHz higher than that of *ntop*. This fit is given in the column $XIAM_{mod}$ of Table I.

IV. RESULTS AND DISCUSSION

A. Comparison of *ntop* and *XIAM*

Using the original version of the program *XIAM*, 378 transitions of 4MAP were fitted with an rms of 99 kHz, about 4 times the measurement accuracy of 25 kHz. The program *ntop* and the modified version of the program *XIAM* reduced the rms deviation to 26 kHz and 29 kHz, respectively, both of which are close to the measurement accuracy. The d_2 and D_{JK} centrifugal distortion constants cannot be determined well. Therefore, they were fixed to the calculated values. We notice that the signs of D_K and d_1 in *XIAM* and *ntop* are opposite. While the sign and value of D_K obtained from *ntop* agree well with the quantum chemically predicted ones, those of d_1 from *XIAM* agree better. The large deviations in D_K in XIAM suggest that it absorbs some of the internal rotation effects, while D_K in *ntop* seems to be much less affected.

The calculated V_3 potentials of the ring and the acetyl methyl groups are 18.07 cm^{-1} and 452.48 cm^{-1}, respectively. They are of the same order of magnitude as the experimental V_3 values, but lower for both rotors. The barrier heights obtained from *XIAM* and *ntop* agree nicely. Because only transitions in the ground torsional states are available, F_0 strongly correlates with V_3 and was fixed to the calculated values in both the *XIAM* and *ntop* fits. The V_6 contribution to the potential cannot be determined and therefore is also fixed to the calculated value.

The internal rotation parameters (V_3, δ, V_K, $D_{\pi^2 K}$, and D_{c3K}) are much better determined with *ntop* than with *XIAM*. In the *XIAM* and $XIAM_{mod}$ fits, the $D_{\pi^2 K}$ parameter also differs significantly, likely due to a correlation with the parameter D_{c3K} introduced in the latter fit. We suspect a higher correlation between internal rotation parameters in *XIAM* compared to *ntop*, since *XIAM* uses a combined axis system, while *ntop* works exclusively in the principal axis system. Therefore, the D_{c3K} and V_K parameters are comparable, but not equivalent.

The *B* and *C* rotational constants deduced from *XIAM* and *ntop* are similar, but the *A* rotational constant obtained from *XIAM* is quite different from that of *ntop*, while the value remains almost the same in fit *XIAM* and fit $XIAM_{mod}$. In the study on 2,4-dimethylanisole, the V_J, V_K, and V_- parameters were also used in *ntop*, resulting in *A*, *B*, and *C* rotational constants that differ significantly from those of *XIAM*.[23] This strongly indicates that the *A* constant is correlated differently with the V_K parameter in *ntop* than it is with the D_{c3K} parameter in *XIAM*.

B. Discussion on the methyl torsional barriers

The V_3 potential for the ring methyl group in 4MAP (**7**) agrees remarkably in the *XIAM* and *ntop* fits, despite the fact that very different fitting approaches are used. The value of approximately 22 cm^{-1} is close to the value of about 28 cm^{-1} found for *p*-tolualdehyde (**5**) (for molecule numbering, see Fig. 1) and the value of about 18 cm^{-1} found for *p*-cresol (**4**), but much lower than the value found for *p*-methylanisole (**8**). As mentioned in the Introduction and discussed in Ref. 23, the less the C_{2v} symmetry of the phenyl frame is broken while substituting the *para*-position of toluene, the lower the V_3 contribution to the potential becomes. In *p*-toluic acid (**6**), the COOH group is almost C_{2v} symmetric. Therefore, the V_6 contribution is the leading term and significantly larger than V_3. In 4MAP (**7**), *p*-cresol (**4**), and *p*-tolualdehyde (**5**), the *para*-substituent of toluene is more C_{2v} symmetric than that in *p*-methylanisole (**8**) (OH ≈ O=C−CH_3 ≈ CHO < O−CH_3), and the V_3 term found for the ring methyl group of *p*-methylanisole is consequently larger [18.39(3) cm^{-1} (**4**) ≈ 21.744 98(6) cm^{-1} (**7**) ≈ 28.111(1) cm^{-1} (**6**) < 49.6370(1) cm^{-1} (**8**)].

For aliphatic ketones, Andresen *et al.* proposed a two-class concept linking the acetyl methyl torsional barrier to the conformational geometry, where molecules in the C_1 class always show a torsional barrier of around 240 cm^{-1}. In this class, the γ carbon of the alkyl chain tilts out of the C-(C=O)−C plane to a synclinal position. The C_s class comprises ketones with "pseudo-C_s" structures in which the torsional barrier of the acetyl methyl group is always around 180 cm^{-1}. In ketones such as 4MAP, a phenyl ring is attached to one side of the carbonyl group, and 4MAP does not belong to either of the two classes mentioned in Ref. 14, probably due to π-electron conjugation between the carbonyl group and the phenyl ring. The simplest ketone containing an acetyl group attached to a phenyl ring is acetophenone (**9**), where the acetyl methyl torsion was found to be 627.0(25) cm^{-1}.[12] In the isomers: acetovanillone (**10**) and 6-hydroxy-3-methoxyacetophenone (**11**), the torsional barriers range from about 522–622 cm^{-1}.[13] Although the value of this parameter depends on the respective isomer and conformer, it remains around 600 cm^{-1}. The value of 588.0(37) cm^{-1} found for the acetyl methyl group of 4MAP strongly supports a third class of ketones, where the acetyl methyl torsional barrier is approximately 600 cm^{-1} if a phenyl ring is attached directly at the other side of the carbonyl group (called the "phenyl class"). Although the symmetry of all current molecules in this "phenyl class" is also C_s, the acetyl methyl torsional barrier is significantly higher than the value of 180 cm^{-1} found for molecules in Andresen's C_s class, showing the decisive role of electronic effects from π-conjugation for this parameter in ketones.

A computational study on how differently the substituents contribute to the effective V_6 and V_3 terms of all these molecules is still missing, and elucidating results might come from effective fragment potential (EFP)[47–49] methods. These have the power to separate the different contributions of exchange-repulsion, electrostatics, dispersion, and polarization to the potential surface. The experimental results provided here will be crucial to judge the reliability of these computational methods.

V. CONCLUSIONS

In this study, the performance of *ntop* was compared to the original *XIAM* and the modified *XIAM* codes. For this purpose, the broadband spectrum of 4-methylacetophenone was recorded and fitted to, finally for both programs, near measurement accuracy.

While the original version of *XIAM* shows a large rms deviation of 99 kHz, both the *ntop* and the modified version of *XIAM* programs show fits with similar quality. The deviations are 26 kHz and 29 kHz, respectively. The interplay between separate fits of large amplitude motion species and global fits was crucial for checking and correcting the assignments. The low V_3 potential of about 22 cm^{-1} obtained for the ring methyl group was compared to that of other *para*-substituted toluene derivatives, and the origin of such a low barrier can be explained from the symmetry surrounding the methyl group. The torsional barrier of the acetyl methyl group was compared to that of other substituted acetophenones, which supports a classification of those ketones in the so-called "phenyl class" with a barrier height of about 600 cm^{-1}.

SUPPLEMENTARY MATERIAL

The supplementary material includes definitions of the operators multiplying the $D_{\pi^2 J}$, $D_{\pi^2 K}$, and $D_{\pi^2 -}$ parameters, frequency lists, all *ntop* and *XIAM* fit files, and the *Gaussian 09* output.

ACKNOWLEDGMENTS

The authors gratefully acknowledge support from the Department of Energy Basic Energy Sciences Gas-Phase Chemical Physics program under Grant No. DE-FG02-96ER14656. H.V.L.N. was supported by the Agence Nationale de la Recherche ANR (Project No. ANR-18-CE29-0011). The authors would like to thank Professor Dr. Wolfgang Stahl for providing the *ntop* source code.

REFERENCES

[1] V. V. Ilyushin, Z. Kisiel, L. Pszczókowski, H. Mäder, and J. T. Hougen, "A new torsion–rotation fitting program for molecules with a sixfold barrier: Application to the microwave spectrum of toluene," J. Mol. Spectrosc. **259**, 26–38 (2010).
[2] L. Ferres, H. Mouhib, W. Stahl, and H. V. L. Nguyen, "Methyl internal rotation in the microwave spectrum of *o*-methyl anisole," ChemPhysChem **18**, 1855–1859 (2017).
[3] L. Ferres, W. Stahl, and H. V. L. Nguyen, "Conformational effects on the torsional barriers in *m*-methylanisole studied by microwave spectroscopy," J. Chem. Phys. **148**, 124304 (2018).
[4] L. Ferres, W. Stahl, I. Kleiner, and H. V. L. Nguyen, "The effect of internal rotation in *p*-methyl anisole studied by microwave spectroscopy," J. Mol. Spectrosc. **343**, 44–49 (2018), spectroscopy of Large Amplitude Vibrational Motion, on the Occasion of Jon Hougen's 80th Birthday—Part II.
[5] S. Jacobsen, U. Andresen, and H. Mäder, "Microwave spectra of *o*-fluorotoluene and its ^{13}C isotopic species: Methyl internal rotation and molecular structure," Struct. Chem. **14**, 217–225 (2003).
[6] K. Nair, J. Demaison, G. Wlodarczak, and I. Merke, "Millimeterwave rotational spectrum and internal rotation in *o*-chlorotoluene," J. Mol. Spectrosc. **237**, 137–142 (2006).
[7] J. Rottstegge, H. Hartwig, and H. Dreizler, "The rotational spectrum, structure and barrier V_6 to internal rotation of *p*-fluorotoluene," J. Mol. Struct. **478**, 37–47 (1999).
[8] G. E. Herberich, "Mikrowellenspektrum, hinderungspotential der internen rotation und teilweise r_0-struktur des para-chlortoluols," Z. Nat., A **22**, 761–764 (1967).
[9] E. G. Schnitzler, N. A. Seifert, I. Kusuma, and W. Jäger, "Rotational spectroscopy of *p*-toluic acid and its 1:1 complex with water," J. Phys. Chem. A **121**, 8625–8631 (2017).
[10] H. Saal, J.-U. Grabow, A. H. Walker, J. Hougen, I. Kleiner, and W. Caminati, "Microwave study of internal rotation in *para*-tolualdehyde: Local versus global symmetry effects at the methyl-rotor site," J. Mol. Spectrosc. **351**, 55–61 (2018).
[11] A. Hellweg and C. Hättig, "On the internal rotations in *p*-cresol in its ground and first electronically excited states," J. Chem. Phys. **127**, 024307 (2007).
[12] J. Lei, J. Zhang, G. Feng, J.-U. Grabow, and Q. Gou, "Conformational preference determined by inequivalent n-pairs: Rotational studies on acetophenone and its monohydrate," Phys. Chem. Chem. Phys. **21**, 22888–22894 (2019).
[13] E. J. Cocinero, F. J. Basterretxea, P. Écija, A. Lesarri, J. A. Fernández, and F. Castaño, "Conformational behaviour, hydrogen bond competition and intramolecular dynamics in vanillin derivatives: Acetovanillone and 6-hydroxy-3-methoxyacetophenone," Phys. Chem. Chem. Phys. **13**, 13310–13318 (2011).
[14] M. Andresen, I. Kleiner, M. Schwell, W. Stahl, and H. V. L. Nguyen, "Sensing the molecular structures of hexan-2-one by internal rotation and microwave spectroscopy," ChemPhysChem **20**, 2063–2073 (2019).
[15] P. Groner, S. Albert, E. Herbst, F. C. D. Lucia, F. J. Lovas, B. J. Drouin, and J. C. Pearson, "Acetone: Laboratory assignments and predictions through 620 GHz for the vibrational-torsional ground state," Astrophys. J. Suppl. Ser. **142**, 145–151 (2002).
[16] H. V. L. Nguyen, I. Kleiner, S. T. Shipman, Y. Mae, K. Hirose, S. Hatanaka, and K. Kobayashi, "Extension of the measurement, assignment, and fit of the rotational spectrum of the two-top molecule methyl acetate," J. Mol. Spectrosc. **299**, 17–21 (2014).
[17] V. Van, W. Stahl, and H. V. L. Nguyen, "Two equivalent methyl internal rotations in 2,5-dimethylthiophene investigated by microwave spectroscopy," Phys. Chem. Chem. Phys. **17**, 32111–32114 (2015).
[18] V. Van, J. Bruckhuisen, W. Stahl, V. Ilyushin, and H. V. L. Nguyen, "The torsional barriers of two equivalent methyl internal rotations in 2,5-dimethylfuran investigated by microwave spectroscopy," J. Mol. Spectrosc. **343**, 121–125 (2018), spectroscopy of Large Amplitude Vibrational Motion, on the Occasion of Jon Hougen's 80th Birthday—Part II.
[19] V. Van, W. Stahl, and H. V. L. Nguyen, "The structure and torsional dynamics of two methyl groups in 2-acetyl-5-methylfuran as observed by microwave spectroscopy," ChemPhysChem **17**, 3223–3228 (2016).
[20] M. Tudorie, I. Kleiner, M. Jahn, J.-U. Grabow, M. Goubet, and O. Pirali, "Coupled large amplitude motions: A case study of the dimethylbenzaldehyde isomers," J. Phys. Chem. A **117**, 13636–13647 (2013).
[21] L. Ferres, K.-N. Truong, W. Stahl, and H. V. L. Nguyen, "Interplay between microwave spectroscopy and x-ray diffraction: The molecular structure and large amplitude motions of 2,3-dimethylanisole," ChemPhysChem **19**, 1781–1788 (2018).
[22] L. Ferres, J. Cheung, W. Stahl, and H. V. L. Nguyen, "Conformational effect on the large amplitude motions of 3,4-dimethylanisole explored by microwave spectroscopy," J. Phys. Chem. A **123**, 3497–3503 (2019).
[23] L. Ferres, W. Stahl, and H. V. L. Nguyen, "Low torsional barrier challenges in the microwave spectrum of 2,4-dimethylanisole," J. Chem. Phys. **151**, 104310 (2019).
[24] H. Hartwig, "Mikrowellenspektroskopische untersuchungen und analyse der internen rotation and dimethyloxiranen und dimethylthiiranen," Ph.D. dissertation (Christian-Albrechts-Universität Kiel, 1995).
[25] H. Hartwig and H. Dreizler, "The microwave spectrum of trans-2,3-dimethyloxirane in torsional excited states," Z. Nat., A **51**, 923–932 (1996).
[26] P. Groner, "Effective rotational Hamiltonian for molecules with two periodic large-amplitude motions," J. Chem. Phys. **107**, 4483–4498 (1997).
[27] N. Ohashi, J. Hougen, R. Suenram, F. Lovas, Y. Kawashima, M. Fujitake, and J. Pyka, "Analysis and fit of the Fourier-transform microwave spectrum of the two-top molecule *N*-methylacetamide," J. Mol. Spectrosc. **227**, 28–42 (2004).
[28] M. Tudorie, I. Kleiner, J. Hougen, S. Melandri, L. Sutikdja, and W. Stahl, "A fitting program for molecules with two inequivalent methyl tops and a plane of symmetry at equilibrium: Application to new microwave and millimeter-wave measurements of methyl acetate," J. Mol. Spectrosc. **269**, 211–225 (2011).
[29] V. V. Ilyushin and J. T. Hougen, "A fitting program for molecules with two equivalent methyl tops and C_{2v} point-group symmetry at equilibrium: Application to existing microwave, millimeter, and sub-millimeter wave measurements of acetone," J. Mol. Spectrosc. **289**, 41–49 (2013).
[30] K. R. Nair, S. Herbers, A. Lesarri, and J.-U. Grabow, "Molecular systems with nearly-free internal rotation and nuclear quadrupole coupling: Meta-chlorotoluene," J. Mol. Spectrosc. **361**, 1–7 (2019).

[31]Z. Kisiel, in *Spectroscopy from Space*, edited by J. Demaison *et al.* (Kluwer Academic Publishers, 2001), pp. 91–106.
[32]A. D. Becke, "Density-functional thermochemistry. III. The role of exact exchange," J. Chem. Phys. **98**, 5648–5652 (1993).
[33]C. Lee, W. Yang, and R. G. Parr, "Development of the Colle-Salvetti correlation-energy formula into a functional of the electron density," Phys. Rev. B **37**, 785–789 (1988).
[34]S. H. Vosko, L. Wilk, and M. Nusair, "Accurate spin-dependent electron liquid correlation energies for local spin density calculations: A critical analysis," Can. J. Phys. **58**, 1200–1211 (1980).
[35]F. J. Devlin, J. W. Finley, P. J. Stephens, and M. J. Frisch, "*Ab initio* calculation of vibrational absorption and circular dichroism spectra using density functional force fields: A comparison of local, nonlocal, and hybrid density functionals," J. Phys. Chem. **99**, 16883–16902 (1995).
[36]S. Grimme, J. Antony, S. Ehrlich, and H. Krieg, "A consistent and accurate *ab initio* parameterization of density functional dispersion correction (DFT-D) for the 94 elements H-Pu," J. Chem. Phys. **132**, 154104 (2010).
[37]A. D. Becke and E. R. Johnson, "Exchange-hole dipole moment and the dispersion interaction," J. Chem. Phys. **122**, 154104 (2005).
[38]E. R. Johnson and A. D. Becke, "A post-Hartree–Fock model of intermolecular interactions," J. Chem. Phys. **123**, 024101 (2005).
[39]E. R. Johnson and A. D. Becke, "A post-Hartree-Fock model of intermolecular interactions: Inclusion of higher-order corrections," J. Chem. Phys. **124**, 174104 (2006).
[40]F. Weigend, "Accurate Coulomb-fitting basis sets for H to Rn," Phys. Chem. Chem. Phys. **8**, 1057–1065 (2006).
[41]F. Weigend and R. Ahlrichs, "Balanced basis sets of split valence, triple zeta valence and quadruple zeta valence quality for H to Rn: Design and assessment of accuracy," Phys. Chem. Chem. Phys. **7**, 3297–3305 (2005).
[42]M. J. Frisch, G. W. Trucks, H. B. Schlegel, G. E. Scuseria, M. A. Robb, J. R. Cheeseman, G. Scalmani, V. Barone, B. Mennucci, G. A. Petersson, H. Nakatsuji, M. Caricato, X. Li, H. P. Hratchian, A. F. Izmaylov, J. Bloino, G. Zheng, J. L. Sonnenberg, M. Hada, M. Ehara, K. Toyota, R. Fukuda, J. Hasegawa, M. Ishida, T. Nakajima, Y. Honda, O. Kitao, H. Nakai, T. Vreven, J. A. Montgomery, Jr., J. E. Peralta, F. Ogliaro, M. Bearpark, J. J. Heyd, E. Brothers, K. N. Kudin, V. N. Staroverov, R. Kobayashi, J. Normand, K. Raghavachari, A. Rendell, J. C. Burant, S. S. Iyengar, J. Tomasi, M. Cossi, N. Rega, J. M. Millam, M. Klene, J. E. Knox, J. B. Cross, V. Bakken, C. Adamo, J. Jaramillo, R. Gomperts, R. E. Stratmann, O. Yazyev, A. J. Austin, R. Cammi, C. Pomelli, J. W. Ochterski, R. L. Martin, K. Morokuma, V. G. Zakrzewski, G. A. Voth, P. Salvador, J. J. Dannenberg, S. Dapprich, A. D. Daniels, Ö. Farkas, J. B. Foresman, J. V. Ortiz, J. Cioslowski, and D. J. Fox, Gaussian 09 Revision E.01, Gaussian Inc. Wallingford, CT, 2013.
[43]P. R. Bunker and P. Jensen, *Molecular Symmetry and Spectroscopy* (NRC Research Press, Ottawa, Ontario, Canada, 2006).
[44]N. Hansen, H. Mäder, and T. Bruhn, "A molecular beam fourier transform microwave study of *0*-tolunitrile: ^{14}N nuclear quadrupole coupling and methyl internal rotation effects," Mol. Phys. **97**, 587–595 (1999).
[45]S. M. Fritz, B. M. Hays, A. O. Hernandez-Castillo, C. Abeysekera, and T. S. Zwier, "Multiplexed characterization of complex gas-phase mixtures combining chirped-pulse fourier transform microwave spectroscopy and VUV photoionization time-of-flight mass spectrometry," Rev. Sci. Instrum. **89**, 093101 (2018).
[46]H. M. Pickett, "The fitting and prediction of vibration-rotation spectra with spin interactions," J. Mol. Spectrosc. **148**, 371–377 (1991).
[47]M. S. Gordon, D. G. Fedorov, S. R. Pruitt, and L. V. Slipchenko, "Fragmentation methods: A route to accurate calculations on large systems," Chem. Rev. **112**, 632–672 (2012).
[48]D. Ghosh, D. Kosenkov, V. Vanovschi, C. F. Williams, J. M. Herbert, M. S. Gordon, M. W. Schmidt, L. V. Slipchenko, and A. I. Krylov, "Noncovalent interactions in extended systems described by the effective fragment potential method: Theory and application to nucleobase oligomers," J. Phys. Chem. A **114**, 12739–12754 (2010).
[49]M. S. Gordon, Q. A. Smith, P. Xu, and L. V. Slipchenko, "Accurate first principles model potentials for intermolecular interactions," Annu. Rev. Phys. Chem. **64**, 553–578 (2013).